A QoS Optical Packet Switching System: Architectural Design and Experimental Demonstration

Maria C. Yuang, National Chiao Tung University
Yu-Min Lin, Industrial Technology Research Institute
Ju-Lin Shih, Po-Lung Tien, and Jason J. Chen, National Chiao Tung University
Steven S. W. Lee, National Chung Cheng University
Shih-Hsuan Lin, National Chiao Tung University

ABSTRACT

Optical packet switching has been considered a prominent paradigm for future WDM networks to efficiently support a multitude of applications with diverse quality of service requirements. In this article we present the architectural design and experimental demonstration of a 10 Gb/s QoS optical packet switching system (QOPSS) for WDM networks. It embodies a set of many-to-one space switches, each of which handles the switching solely for a cluster of wavelengths. With the cluster-based optical switch design, QOPSS trades off limited statistical multiplexing gains for higher system scalability. By *many-to-one*, multiple packets that are carried by different internal wavelengths are scheduled to switch to the same output port but receive different delays afterward. QOPSS adopts downsized feed-forward optical buffers, yielding drastic reduction in packet loss probability in an economical manner. Significantly, through using four-wave-mixing wavelength converters at the output section, QOPSS permits optical packet preemption, thus achieving effectual QoS differentiation. The article presents both simulation and experimental testbed results to demonstrate the feasibility and superior packet loss/QoS performance of the system.

INTRODUCTION

Future optical wavelength-division multiplexing (WDM) [1] networks are expected to flexibly and cost-effectively satisfy a multitude of applications with diverse quality of service (QoS) requirements. Such facts bring about the need to exploit the optical packet switching (OPS) [1, 2] paradigm that advocates efficient sharing of wavelength channels among multiple connections. Nevertheless, OPS systems still face several technological limitations, such as optical random access memory (RAM) and optical signal processing. Hence, the OPS system we study in this work employs *almost-all* optical switches in which packet payloads remain in the optical domain, and only the control headers are processed electronically. A general OPS system consists of three basic components that are crucial to the performance and economy of the system: the space switch, optical buffer, and wavelength converter [3]. While the space switch operates as a main subsystem to switch incoming packets to their destined output ports, the optical buffer and wavelength converter help resolve contentions in time and wavelength dimensions, respectively.

First, space switches can be categorized as being non-blocking or blocking [4, 5]. Non-blocking switches are mostly used for traditional electronic circuit switching systems. Non-blocking switches, such as the crossbar matrix network and Cantor network, can always construct a new connection between the input and output ports without altering other connections already in the switches. However, these non-blocking switches are less scalable and economically infeasible in the optical domain due to using a large number of switching elements. There is another type of non-blocking switches, called rearrangeable switches (e.g., Benes network), which route new input-output connections by rearranging all other existing connections. Rearrangeable switches are more scalable than their non-blocking counterparts, but they nevertheless require more complicated scheduling (or rearranging) algorithms, causing the switch processing to slow down. For the second category, blocking switches, Banyan switches enable self-routing and require the least number of switching elements. It is the most scalable and economic architecture, but at the cost of reduced throughput due to the occurrence of internal blocking [4]. In this work, we aim at achieving high scalability of switches by exploiting a set of smaller space switches that can be of any above architecture type.

Second, optical buffers are currently achieved by ether increasing the light path distance via

0163-6804/10/$25.00 © 2010 IEEE

fiber delay lines (FDLs), or slowing down the light velocity. The slow-light technologies [6, 7] have been shown to have limited capacity and delay-bandwidth product [7]. For this reason, the FDL-based optical buffer remains a more practical option. The FDL-based optical buffer can be applied under various buffering strategies [8]: input buffering, output buffering, and shared buffering. While input (output) buffering has a separate buffer for each input (output) port, shared buffering allows buffers to be shared among multiple inputs and/or outputs. There are two major FDL-based buffering structures: feedback or feed-forward [9]. The feedback structure can support dynamic buffering durations at the expense of additional hardware to maintain signal quality [10–12]. By contrast, the feed-forward FDL structure only supports fixed buffering durations [13] but ensures better signal quality. Thus, the feed-forward structure is generally preferred over its feedback-based counterpart.

Third, tunable optical wavelength converters (TOWCs) offer an alternative to contention resolution in the space (wavelength) dimension. Because TOWCs impose a high cost penalty on OPS systems, much research work has focused on the reduction of the cost via the sharing of TOWCs [14] and/or the use of limited-range TOWCs [15]. In general, TOWCs can be realized by three key methods [15]: cross-gain modulation (XGM), cross-phase modulation (XPM) [16], and four-wave mixing (FWM) [17]. By taking advantage of the gain saturation phenomenon of the semiconductor optical amplifier (SOA), the XGM scheme inversely transfers the modulation of the input wavelength's amplitude to that of the output wavelength's amplitude. The scheme is simple and polarization-insensitive due to the use of the polarization-insensitive SOA. However, its major drawback is the reduction of the extinction ratio for up-converted signals. In the XPM scheme, the refractive index of one arm of the SOA-integrated interferometer is modulated in accordance with the source signal's intensity. As a result, the two-arm XPM converter generates either a constructive or destructive interference effect on the target wavelength. Such an effect entails the encoding of the source bitstream onto the target wavelength. The scheme outperforms XGM in the extinction ratio and conversion range at the cost of more complex components. Nevertheless, XPM converters are limited to amplitude modulation formats and require accurate control of the SOA bias [15]. Finally, an FWM converter is based on the four-wave-mixing nonlinear effect of SOA for converting wavelengths. The FWM scheme is attractive because of being able to convert a group of wavelengths simultaneously, and transparent to the modulation format and data rate. With the method proposed in [17], the FWM converter can attain high conversion efficiency even for large conversion ranges.

In this article we present the architectural design and experimental demonstration of a 10 Gb/s QoS-enabled optical packet switching system (QOPSS) for WDM networks. QOPSS boasts three crucial features. First, it embodies a set of many-to-one space switches, each of which handles the switching solely for a cluster of wavelengths. Such cluster-based optical switch design aims at trading off limited statistical multiplexing gains for higher system scalability. Second, QOPSS adopts downsized feed-forward optical buffers that are applied based on the output and shared buffering strategies. Such a design, as shown herein, yields drastic reduction in packet loss probability (PLP) in an economical fashion. Third, by incorporating FWM converters at the output section, QOPSS supports *optical packet preemption* by permitting higher-priority packets to preempt lower-priority packets already in the delay lines, thereby achieving effectual QoS differentiation. Finally, the article presents both simulation and experimental testbed results to demonstrate the viability and superior packet loss/QoS performance of the system.

The remainder of this article is organized as follows. In the next section we present the general architecture of QOPSS. The operations of packet switching, buffering, and preemption are detailed. We then display via simulation results the packet loss and QoS performance of QOPSS. We then delineate the experimental testbed system setup, and demonstrate the performance of system components and the feasibility of QOPSS. Finally, concluding remarks are given in the final section.

A general OPS system consists of three basic components that are crucial to the performance and economy of the system: the space switch, optical buffer, and wavelength converter. While the space switch operates as a main subsystem to switch incoming packets to their destined output ports, the optical buffer and wavelength converter help resolve contentions in time and wavelength dimensions, respectively.

QOPSS: System Architecture

QOPSS is a synchronous system that supports fixed-size packets of different priorities. As shown in Fig. 1, it consists of two parts: the optical switch and the central switch controller (CSC). First, before entering the optical switch, all packets are required to be time-aligned (synchronous). Such synchronization can be implemented by the use of cascaded switched fiber delay lines [18, 19]. While each packet header that carries the label and QoS (priority) information is electronically processed by the CSC, the payload travels within the switch all-optically. The header is modulated with its payload based on the superimposed amplitude shift keying (SASK) technique [20].

The optical switch consists of four sections: input, many-to-one space switch (MOSS), output buffer, and output sections. In the input section there are N input fibers, each carrying W wavelengths. After demultiplexing, for each packet a TOWC converts its input wavelength to an internal wavelength that corresponds to a free space in the output optical buffer. In the MOSS section there are c independent space switches that are responsible for switching c clusters of wavelengths, respectively. Each space switch is a broadcast-and-select-based switch. Specifically, space switch SS_k switches W/c input wavelengths (from $\lambda_{(k-1)W/c+1}$ to $\lambda_{kW/c}$), for each of N fibers, to W/c output wavelengths (from $\lambda_{(k-1)W/c+1}$ to $\lambda_{kW/c}$), lending the switch size to $N \cdot (W/c) \times N \cdot (W/c)$, where c is the total number of clusters in the switch. Notice that by *many-to-one*, multiple packets coming from different inlets that are scheduled to depart from the system through the same output wavelength and fiber but receiving different delays are carried by different internal wavelengths and switched to the same outlet.

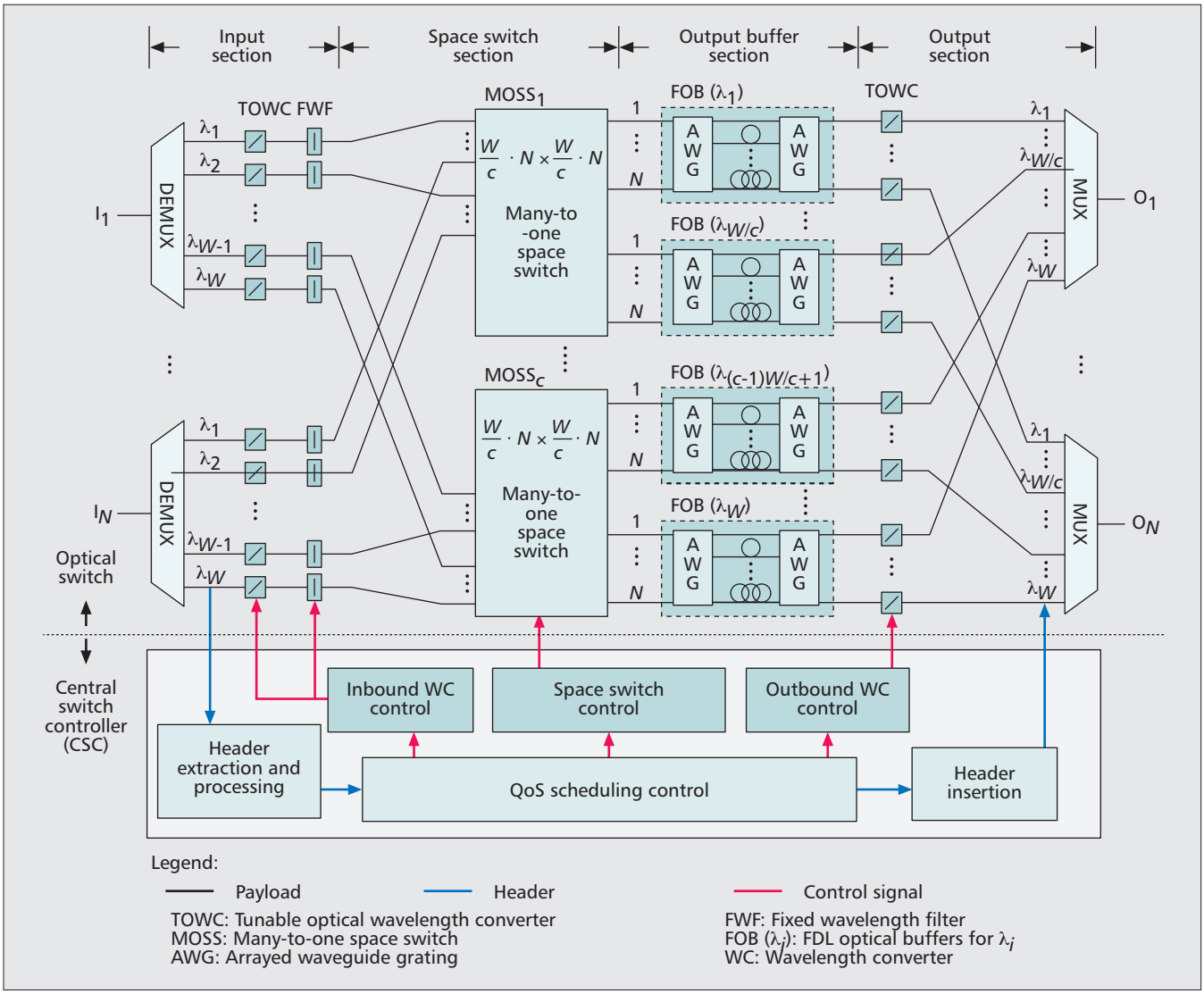

Figure 1. *QOPSS: system architecture.*

The output buffer section contains W FDL optical buffers (FOBs) for W wavelengths, respectively. Each FOB is shared by all N output ports. An FOB is composed of a pair of arrayed waveguide gratings (AWGs) and F optical FDLs connecting the AWGs, resulting in a total of BF buffer positions, where $BF = (F - 1) \times M$, and M is the number of internal wavelengths. It is worth noting that a packet entering the FOB at the ith input port will exit the buffer from the ith output port after receiving a certain delay time determined by the internal wavelength [12]. Thus, for any FOB, an internal wavelength of a packet uniquely determines the delay received by the packet. In the output section there are $N \times W$ FWM-based TOWCs and N output fibers, each carrying W wavelengths. At each output port of the second AWG of an FOB, multiple packets that are carried by different internal wavelengths may have been scheduled to exit from the output port at the same time. This only occurs as a result of an attempt to preempt a lower-priority packet that has already been in the delay line by a higher-priority packet observing unavailable buffer space upon arrival. The preemption is accomplished by tuning the FWM converter in such a way that, upon converting the group of wavelengths, the target wavelength for the high-priority packet falls into the output wavelength. Then all other packets outside of the output wavelength are automatically dropped after the multiplexing.

The CSC is composed of six modules. The headers of newly arriving packets are first demodulated [20] by the header extraction and processing module. Their label and priority information is passed to the QoS scheduling control module. The module performs QoS scheduling by determining the destined wavelength and the internal wavelength corresponding to the buffer delay that each packet is going to receive. Basically, packets are sequentially scheduled based on the following simple algorithm, which adopts priority upon arrival with preemption (PA+P): high-priority packets receive lower delay than low-priority packets; and if the system is full, a newly arriving high-priority packet can preempt the low-priority packet in the buffer receiving the least delay. Due to the clustering-based architecture design,

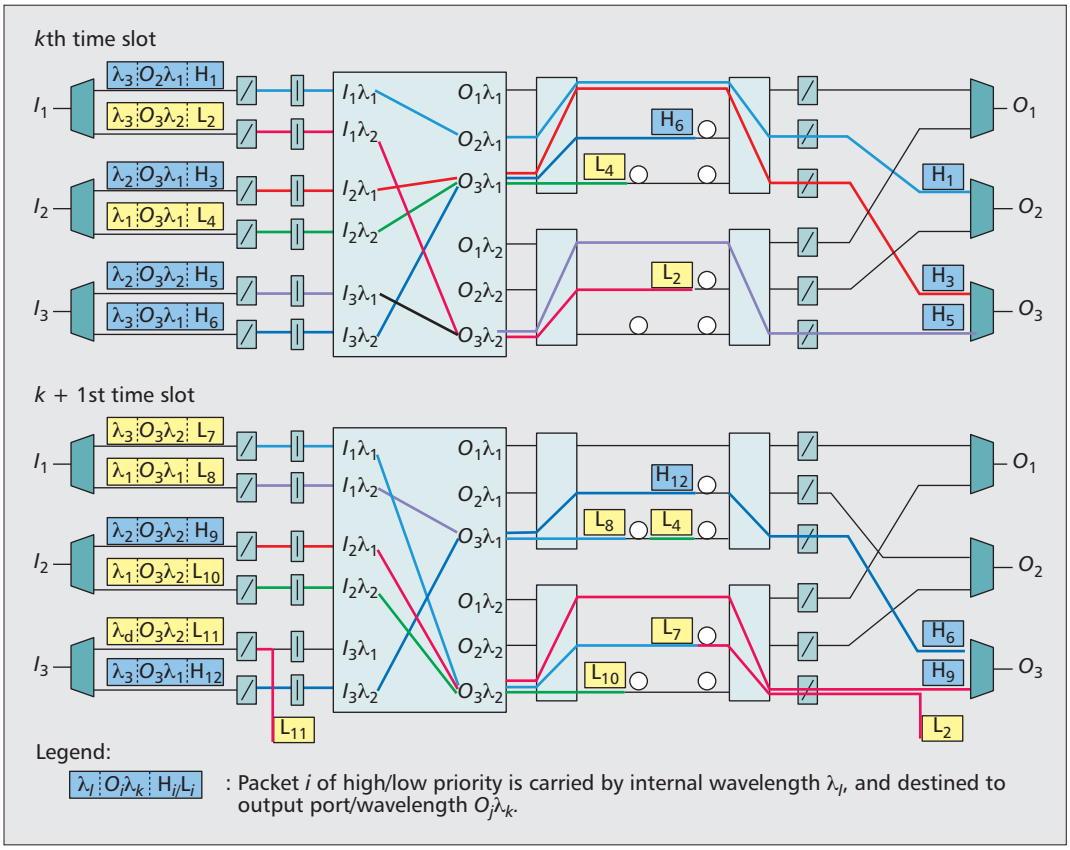

Figure 2. *Packet switching, buffering, and preemption - an example.*

The preemption is accomplished by tuning the FWM converter in such a way that, upon converting the group of wavelengths, the target wavelength for the high-priority packet falls into the output wavelength. Then, all other packets outside of the output wavelength are automatically dropped after the MUX.

packet scheduling for all clusters can be performed independently and in parallel. The computational complexity of the scheduling algorithm is polynomially bounded and can be derived as follows. Given that there are at most $N(W/c)$ packets in each cluster, and each packet is sequentially assigned with one output wavelength (out of W/c wavelengths) and one fiber delay line/internal wavelength in the FOB (out of F FDL's), the computational complexity is thus $O(N(W/c)^2F)$. Regarding scheduling algorithms, in another line of our work in which the broadcast-and-select space switches are economically replaced by pseudo-Banyan space switches, a near-optimal packet scheduling algorithm [21] was proposed to solve the NP-complete packet scheduling problem.

The QoS control module then passes the destined wavelength/output port, internal wavelength, and preemption information to the space switch (SS) control, inbound wavelength converter (WC) control, and outbound WC control modules, respectively. Finally, the header insertion module inserts and combines the new header with its payload before exiting from the optical switch.

We now illustrate the packet switching, buffering, and preemption operations via an example, as shown in Fig. 2. In this example the system has three input/output ports and two input/output wavelengths. It uses three internal wavelengths corresponding to three FDLs of no, one-slot, and two-slot delays, respectively. There are six packets that arrive at each of the kth and k + 1st time slots, of which six are of high priority (H) and six of low priority (L). At the kth slot, high-priority packets H_1, H_3, and H_5 are switched directly to their destined output ports without experiencing any delay. The remaining three packets (L_2, L_4, and H_6) are switched and buffered in the FDLs, as shown in the figure. For example, L_2 is destined to $O_3\lambda_2$, which is occupied by H_5 and becomes unavailable. The system then tags L_2 with internal wavelength λ_3 so that the packet can be inserted to the delay line with one-slot delay. At the k + 1st slot, packet H_9 arrives and is scheduled to pass through the system by preempting L_2 in the buffer due to having a full buffer. To this end, H_9 is tagged with interval wavelength λ_2 and departs from the buffer simultaneously with L_2, with the result that L_2 is dropped before multiplexing. Besides, due to unavailable buffer space, L_{11} is immediately discarded before entering the system.

PLP and QoS Differentiation: Simulation Results

Recall that each MOSS is a broadcast-and-select non-blocking switch; packets are only lost due to unavailable optical buffers. In this section we examine the PLP and QoS performance of QOPSS under different numbers of wavelengths (per cluster), numbers of FDLs, and traffic burstiness via simulation results. We carried out a time-based simulation implemented in C++. Simulation terminated after reaching a 95 percent confidence interval. In the simulation each

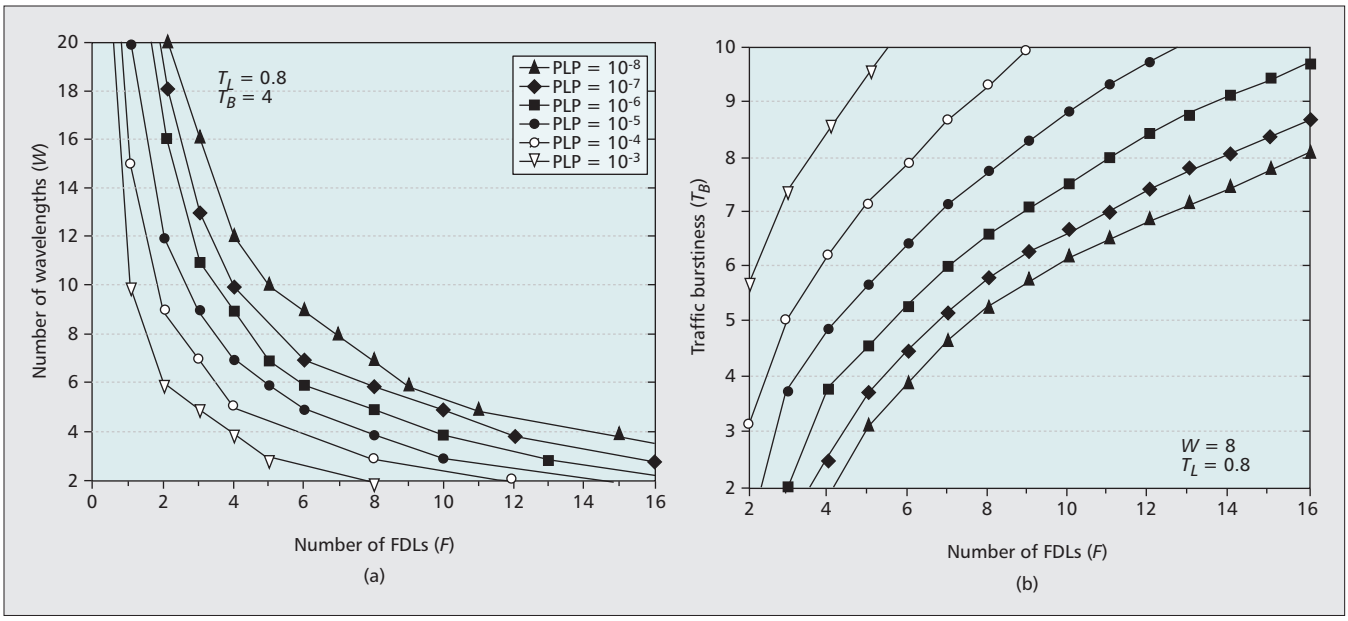

Figure 3. *Packet loss probability (PLP) guarantees under various system and traffic settings: a) wavelength and FDL numbers requirements; b) FDL number requirement under various burstiness.*

MOSS handles a total of 10 input/output ports and W wavelengths, resulting in $10W$ connections processed by the MOSS. Each connection is given an identical load of traffic generated following a two-state interrupted Bernoulli process (IBP) [22] for modeling busty traffic. The two states are the 1 and 0 states, which correspond to high and low mean arrival rates, respectively. The IBP is characterized by four parameters (α, β, λ_1, λ_0), where the high-to-low-state transition probability is equal to $\alpha = 0.225$, and the low-to-high-state transition probability is equal to $\beta = 0.025$. Accordingly, the mean traffic load (T_L) can be expressed as $(\beta \times \lambda_1 + \alpha \times \lambda_0)/(\alpha + \beta)$, and traffic burstiness (T_B) can be given by the ratio of the peak rate to the mean rate (i.e., λ_1/T_L). Traffic destination is uniformly distributed among all output ports. Simulation results are shown in Fig. 3.

In Fig. 3a we depict the joint requirement of the total number of wavelengths and the number of FDLs for achieving various grades of PLP. For instance, to achieve a PLP of 10^{-8} requires 16 wavelengths and 3 FDLs or 8 wavelengths and 7 FDLs. This result reveals that for this example, to achieve greater scalability with two clusters (an 8×8 vs. 16×16 switch), the system can achieve the same loss performance by using a marginally greater FDL number (7 vs. 3). Besides, with the same number of wavelengths, applying only a few optical buffers immediately yields drastic improvement in PLP, as indicated by the large slopes when the buffer size is small. This fact justifies the economical use of a downsized optical buffer in our system. In Fig. 3b, we delineate the number of FDLs that is required for the guarantees of different grades of PLP under various traffic burstiness. We observe that, given any buffer size, the greater the burstiness, the poorer the loss probability. The result provides a guideline on the requirements of the number of FDLs for achieving an acceptable grade of PLP under any given traffic burstiness.

We further demonstrate the provision of QoS differentiation in terms of packet loss performance. In the simulation, among the $10W$ connections, there are two priorities (H and L) contributing the same amount of traffic load. All other parameter settings are identical to those described above. We draw a comparison of PLP among four following QoS scheduling schemes:

- No priority (NP)
- Priority upon arrivals (PA)
- QoS scheduling for QOPSS (i.e., priority upon arrivals with preemption [PA+P])
- Head-of-line priority (HOL)

While the PA scheme provides an entry-level priority where priority takes effect only upon arrival, the HOL scheme is portrayed as an ideal one that gives absolute priority to high-priority packets at all times. Note that the HOL scheme cannot be realized for optical networks with non-circulated FDL-based buffers, and is used solely for comparison purposes. Simulation results are shown in Fig. 4.

In Fig. 4 we display PLP as a function of increased low-priority and high-priority traffic loads in Figs. 4a and 4b, respectively. With the ideal HOL scheme, the loss probability of high-priority packets remains completely unaffected by the increasing low-priority loads. We discover from Fig. 4a that our scheme (PA+P) incurs slightly deteriorating loss probability but outperforms the PA and NP schemes by several orders of magnitude. When the high-priority traffic load increases (Fig. 4b), all four schemes undergo deteriorating loss probability. Nevertheless, compared to the NP and PA schemes, our scheme (PA+P) yields drastic improvement in loss probability due to the preemption feature. In Figs. 4c and 4d we focus on the loss probability of our PA+P scheme under different optical buffer sizes and traffic loads. As shown in the figures, even though our scheme exhibits inferior loss probability compared to the ideal HOL case, such inferiority can be cost-effectively compen-

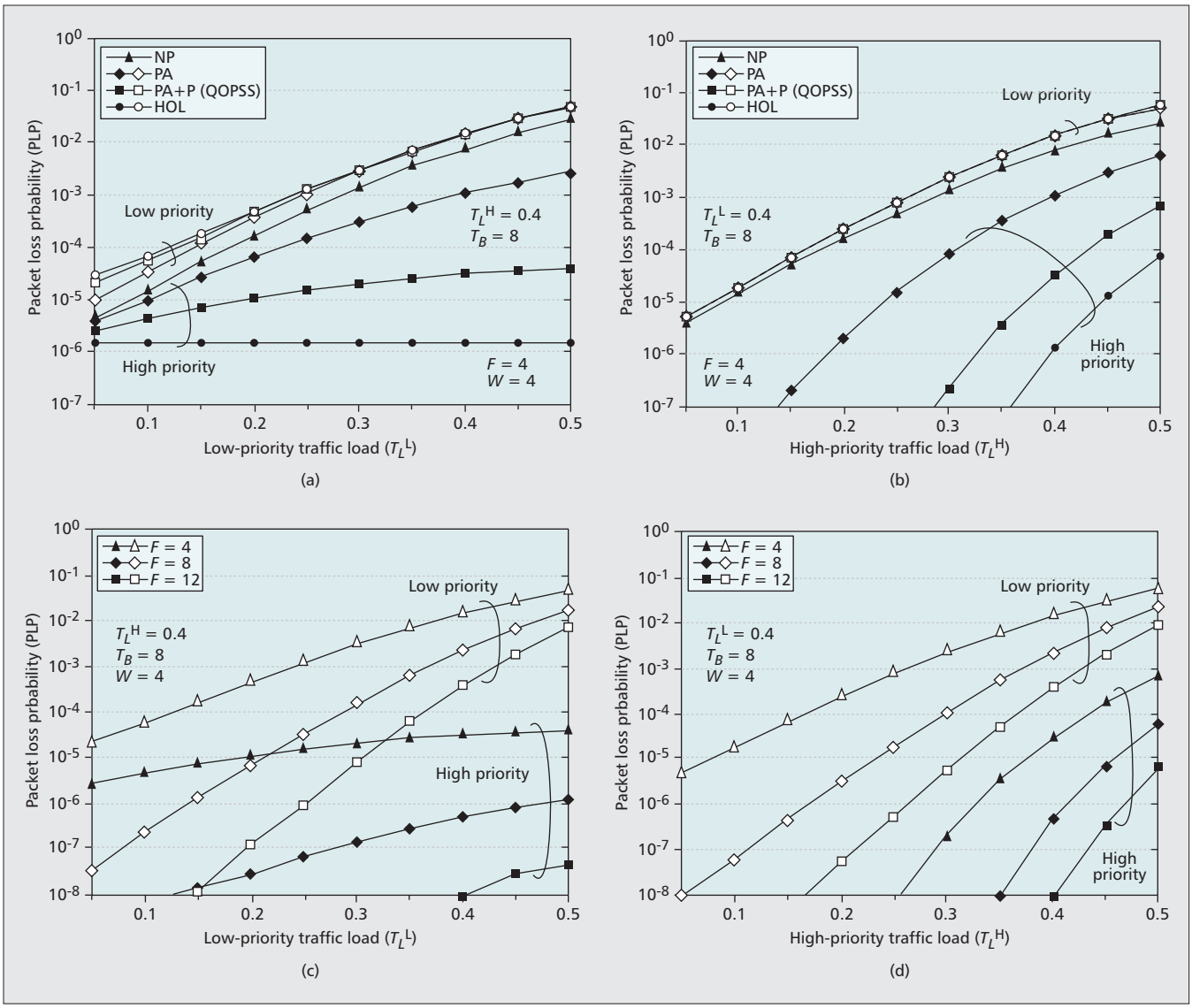

Figure 4. *Comparisons of different QoS scheduling schemes with respect to packet loss probability: a) four QoS schemes: fixed high-priority load; b) four QoS schemes: increasing high-priority load; c) PLP of QOPSS: fixed high-priority load; d) PLP of QOPSS: increasing high-priority load.*

sated for by using slightly larger buffers. We observe that, due to the preemption feature, QOPSS achieves superior QoS differentiation by offering high-priority traffic lower loss probability by several orders of magnitude than that of low-priority traffic.

Experimentation Setup and Results

To demonstrate the feasibility and performance of QOPSS, we have implemented an experimental testbed, as shown in Fig. 5. The testbed operates at a data rate of 10 Gb/s and is time-slotted with each slot 2 μs long. Without loss of generality, we only implement one signal path in the optical switch, as shown in the upper part of Fig. 5. In the control plane a field-programmable gate array (FPGA)-based traffic generator produces four traffic channels using two labels and two priorities. For each channel, the traffic arrivals are generated following an IBP described above. The first-channel traffic is used to trigger the 10 Gb/s pulse pattern generator (PPG) to actually pump out packets. The remaining three channels' information is passed to the CSC to virtually emulate desired traffic and loads. The FPGA-based CSC reads the label information and schedules packets (by determining the optical data path) according to the QoS scheduling control algorithm (PA+P). The optical data path is uniquely determined by the input and output wavelengths, and a path in the two-by-two MOSS. The CSC then sends the wavelength information to the tunable laser controllers, which contain lookup tables of the currents for controlling the three-section distributed Bragg reflector (DBR) tunable laser diodes in IWC and OWC. The CSC also sends four on/off signals to the SOAs, setting up the path in the MOSS. In the meantime, the CSC updates the mean packet loss rate periodically displayed on a PC.

In the optical data path, the channels of the

In the control plan an FPGA-based traffic generator produces four traffic channels using two labels and two priorities. For each channel, the traffic arrivals are generated following an IBP. The first-channel traffic is used to trigger the 10 Gb/s pulse pattern generator to actually pump out packets. The remaining three channels' information is passed to the CSC to virtually emulate desired traffic and loads.

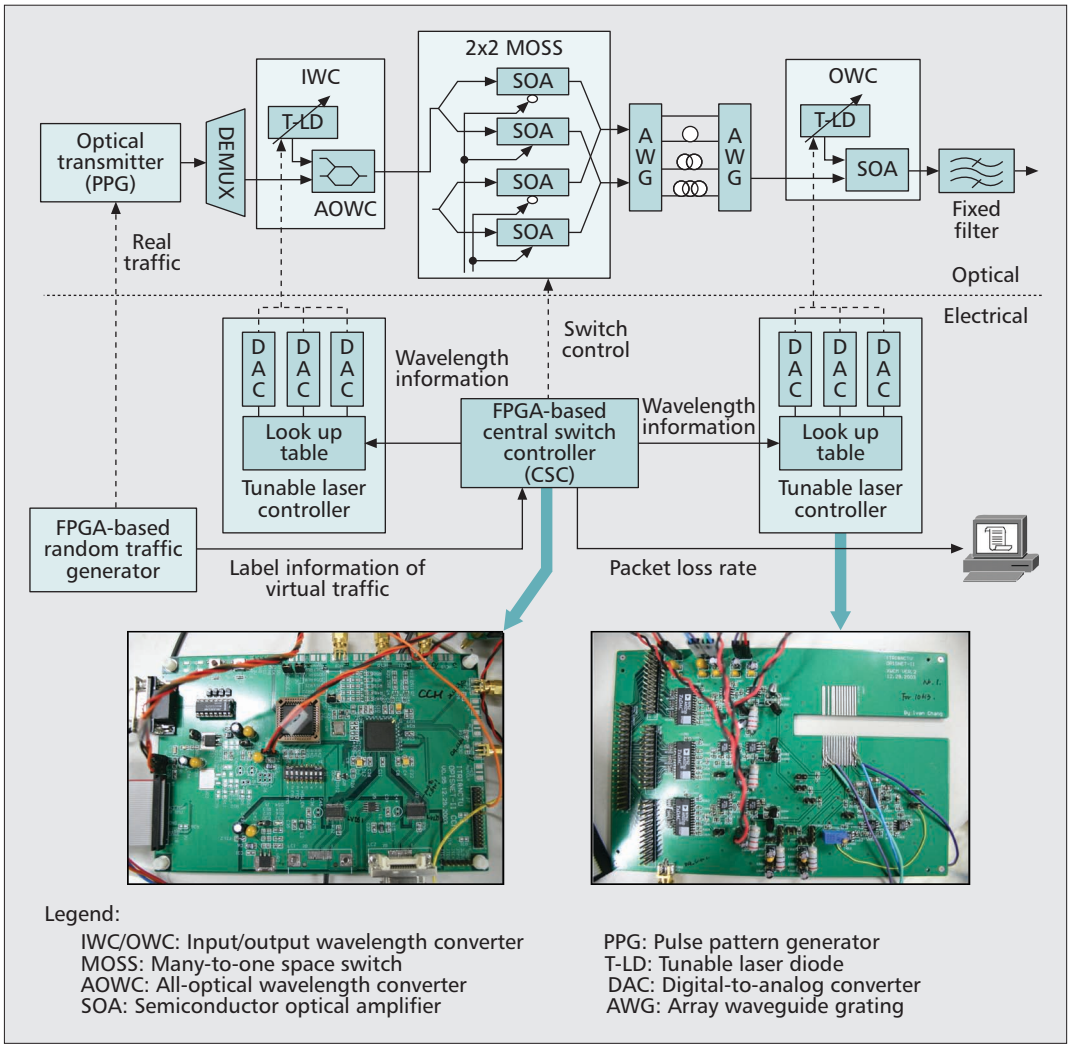

Figure 5. *Experimental setup of the QOPSS testbed.*

input fiber port are first demultiplexed and passed to input wavelength converters. The input wavelength used in the experiment is 1550.92 nm. Based on the XPM technique, the input wavelength converter is implemented by a fast DBR tunable laser and Mach-Zehnder interferometer [23]. The signal on the input wavelength (1550.92 nm) is converted to one of four AWG internal wavelengths (1544.13 nm, 1545.72 nm, 1550.52 nm, and 1552.12 nm), which correspond to 0, 1-packet (2 μs), 2-packet (4 μs), and 3-packet (6 μs) delays, respectively, to be received later in the fiber delay lines.

Packets are passed to the MOSS implemented by four SOAs that function as on/off gates in addition to four fiber couplers. Provided with a 140 mA switching current to each SOA, the MOSS achieves a switching time less than 50 ns and an on/off extinction ratio greater than 30 dB. Packets then pass through the designated FDL determined by the internal wavelength. The FDLs serve as a shared buffer that incorporates two cyclic AWGs as input and output stages. Multiple packets that depart from the same output port of the AWG are simultaneously converted via the four-wave-mixing (FWM)-based [17] wavelength converter with a conversion efficiency of 10 dB. The desired output wavelength in the experiment is 1540.56 nm. Packets that are outside of this wavelength are preempted and dropped after passing through the fixed optical filter (or multiplexer).

Experimental results are shown in Fig. 6. Recall that the response speed of the XPM-based wavelength converter is determined by the tunable laser's tuning time, which is less than 200 ns in our case, as shown in Fig. 6a. With the open eye diagram shown in the inset, we demonstrate that the signal integrity is finely maintained after the converter. For the AWG optical buffer, the average insertion loss of an AWG is 4 dB. As displayed in Fig. 6b, the transmission spectrum of the AWG retains uniform power loss across all wavelengths. Next, we present the functional diagram of the FWM converter in Fig. 6c. The converter generates the FWM phenomenon using two tunable pump lasers (TL-P1 and TL-P2) along with the input wavelength, and an additional assisted beam injected into the SOA. As indicated by the bit error rate (BER) curves in Fig. 6c, the use of an additional assisted beam yields a significant improvement in the conversion efficiency. For both up and down conversions, the results show that our converter

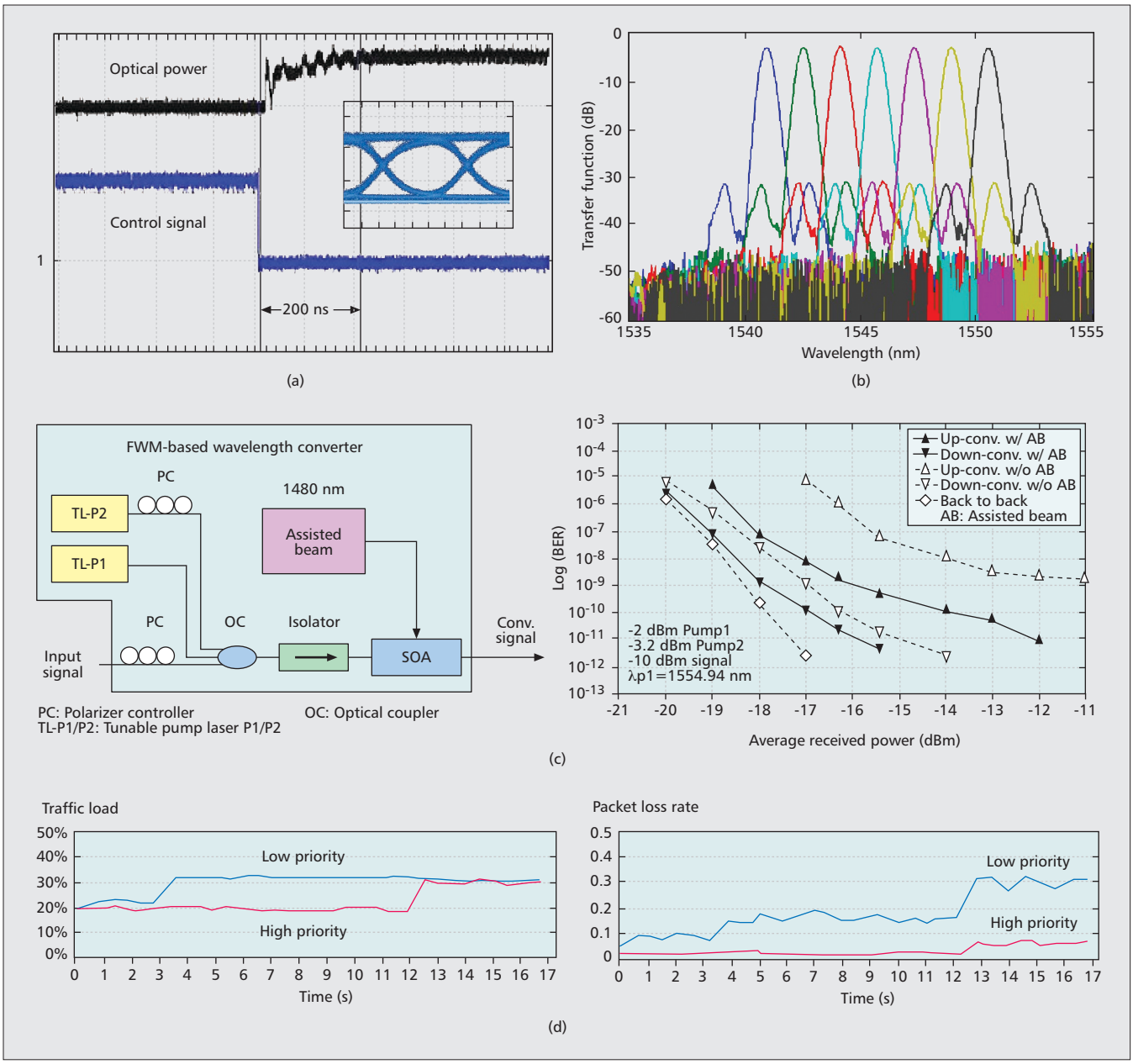

Figure 6. *Experimental testbed results: a) cross-phase-modulation (XPM) converter; b) AWG optical buffer; c) FWM-based wavelength converter and its performance (conversion range = 25 nm); d) traffic load and resulted mean packet loss rate over time.*

with the assisted beam achieves much lower BER than that without the assisted beam. Finally, we depict the mean packet loss rate over time according to a given traffic load scenario in Fig. 6d. In this scenario, the low-priority traffic load is first increased at the third second, followed by an increase of the high-priority traffic load at the 12th second. Testbed results show that low-priority traffic suffers a higher loss rate immediately after the third second. However, high-priority traffic experiences unaffected loss rate until the 12th second. It then inevitably undergoes higher loss rate after the 12th second when the traffic load of the same class has increased. Meanwhile, low-priority traffic suffers worsening packet loss rate as a result of more preemption by high-priority traffic.

We next demonstrate packet preemption in Fig. 7 with experimental testbed results. The scenario for the experiment is illustrated in Fig. 7a. For the scenario, Fig. 7b contains the traces that are taken from the digital waveform scope showing the presence of packets at five different stages (i to v) of the system. In the scenario, the system has a buffer size of two in addition to the zero-delay delay line. Prior to the kth time slot, there are two packets in the buffer: low-priority packet 1 (L_1) and high-priority packet 2 (H_2). At the kth time slot, two new packets (packets H_3 and L_4) arrive at the system. Due to being able to accommodate at most three packets, H_3 is scheduled to preempt L_1, which is going to depart from the system at the next time slot. In addition, packet L_4 is scheduled to be placed at the end of the buffer. To this end, H_3 is set with the internal wavelength so that it can

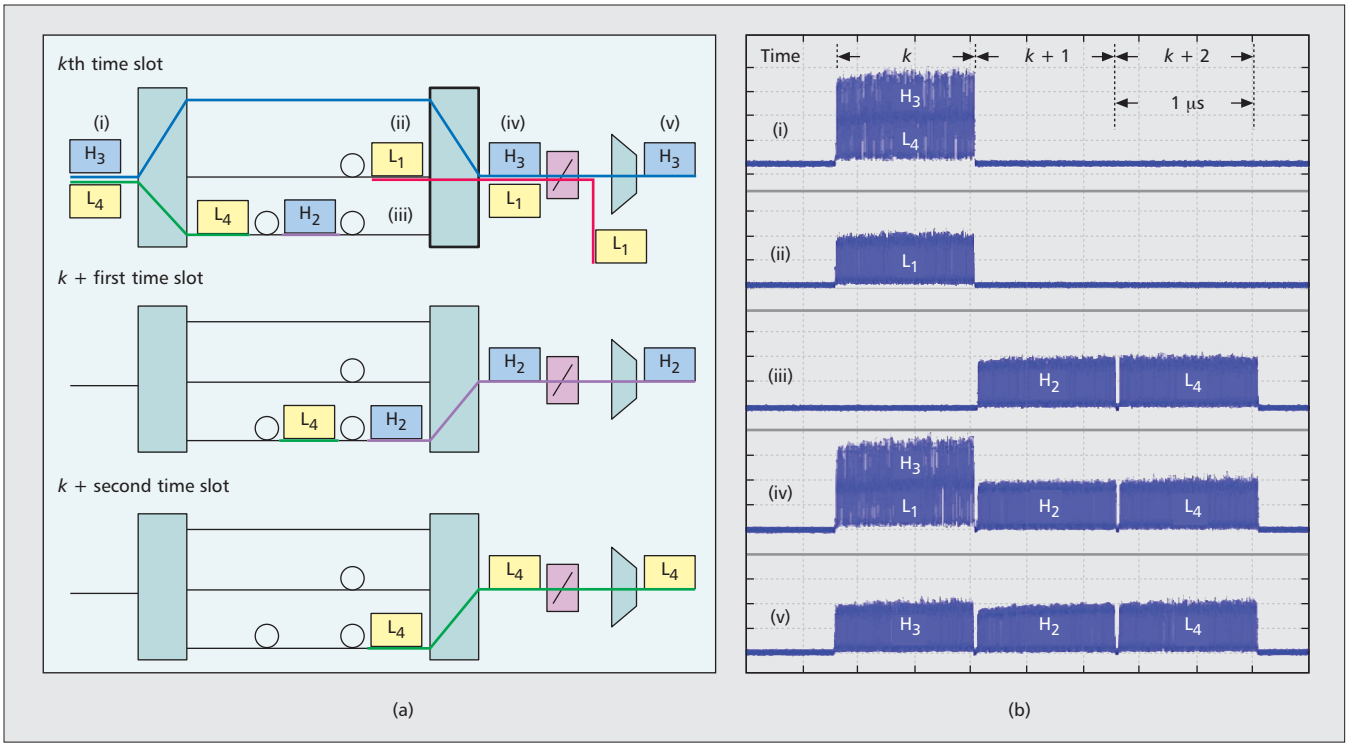

Figure 7. *Demonstration of packet preemption: a) the scenario; b) traces displayed in optical scope.*

travel through the buffer with no delay. As expected, both packets H_3 and L_1 depart from the buffer at the *k*th time slot simultaneously. This is shown in stage iv in Fig. 7b by the waveform's amplitude, which is twice as high as that of a single-packet. The FWM-based wavelength converter is tuned so that H_3's wavelength matches the output wavelength, 1540.56 nm. As a result, packet H_3 is passed where packet L_1 is blocked by the multiplexing filter after the converter, shown in stage v in Fig. 7b. Finally, packet L_4 exits from the system at the k + 2nd time slot. From the scope traces in Fig. 7b, we observe that QOPSS provides packet buffering and preemption in a fully precise and synchronous manner.

Conclusions

In this article we have presented the architectural design and experimental testbed demonstration of QOPSS, a 10 Gb/s QoS optical packet switching testbed system for WDM networks. The architecture of QOPSS includes XPM wavelength converters, MOSSs, AWG-based optical buffers, and FWM wavelength converters for the optical switching, buffering, and preemption of packets. We show simulation results to emphasize that to achieve higher system scalability with more space-switch clusters, QOPSS can guarantee the same grade of PLP by using a marginally larger buffer size, revealing the economic use of a handful of optical buffers. As a result of the preemption feature, QOPSS was shown to achieve superior QoS differentiation by offering high-priority traffic lower loss probability by several orders of magnitude than that of low-priority traffic. Experimental results demonstrated that the system components achieve high signal integrity, uniform signal power, and low bit error rate, justifying the feasibility of the system. Finally, we observe from the waveform scope that, for a given scenario, the QOPSS testbed system precisely and synchronously performed the switching, buffering, and preemption of packets.

References

[1] M. Yuang *et al.*, "HOPSMAN: An Experimental Testbed System for a 10 Gb/s Optical Packet-Switched WDM Metro Ring Network," *IEEE Commun. Mag.*, vol. 46, no. 7, July 2008, pp. 158–66.

[2] M. Yuang *et al.*, "Optical Coarse Packet-Switched IP-over-WDM Network (OPSINET): Technologies and Experiments," *IEEE JSAC*, vol. 24, no. 8, Aug. 2006, pp. 117–27.

[3] G. Papadimitriou, C. Papazoglou, and A. Pomportsis, "Optical Switching: Switch Fabrics, Techniques, and Architectures," *J. Lightwave Tech.*, vol. 21, no. 2, Feb. 2003, pp. 384–405.

[4] S. Li, *Algebraic Switching Theory and Broadband Applications*, Academic Press, 2001.

[5] A. Jajszczyk, "Nonblocking, Repackable, and Rearrangable Clos Networks: Fifty Years of the Theory Evolution," *IEEE Commun. Mag.*, vol. 41, no. 10, Oct. 2003, pp. 28–33.

[6] G. Chang *et al.*, "Enabling Technologies for Next-Generation Optical Packet-Switching Networks," *Proc. IEEE*, vol. 94, no. 5, May 2006, pp. 892–910.

[7] R. Tucker, P. Ku, and C. Hasnain, "Slow-Light Optical Buffers: Capabilities and Fundamental Limitations," *J. Lightwave Tech.*, vol. 23, no. 12, Sept. 2005, pp. 4046–66.

[8] S. Dixit, *IP over WDM: Building the Next Generation Optical Internet*, Wiley, 2004.

[9] M. Chia *et al.*, "Packet Loss and Delay Performance of Feedback and Feed-Forward Arrayed-Waveguide Gratings-Based Optical Packet Switches With WDM Inputs-Outputs," *J. Lightwave Tech.*, vol. 19, no. 9, Sept. 2001, pp. 1241–54.

[10] Z. Zhang and Y. Yang, "Low-Loss Switching Fabric Design for Recirculating Buffer in WDM Optical Packet Switching Networks Using Arrayed Waveguide Grating Routers," *IEEE Trans. Commun.*, vol. 54, no. 8, Aug. 2006, pp. 1469–72.

[11] S. Liew, G. Hu, and H. Chao, "Scheduling Algorithms for Shared Fiber-Delay-Line Optical Packet Switches — Part I: The Single-State Case," *J. Lightwave Tech.*, vol. 23, no. 4, Apr. 2005, pp. 1586–1600.
[12] F. Choa *et al.*, "An Optical Packet Switch Based on WDM Technologies," *J. Lightwave Tech.*, vol. 23, no. 3, Mar. 2005, pp. 994–1014.
[13] T. Zhang, K. Lu, and J. Jue, "Shared Fiber Delay Line Buffers in Asynchronous Optical Packet Switches," *IEEE JSAC*, vol. 24, no. 4, Apr. 2006, pp. 118-127.
[14] V. Eramo, M. Listanti, and M. Spaziani, "Resources Sharing in Optical Packet Switches with Limited-Range Wavelength Converters," *J. Lightwave Tech.*, vol. 23, no. 2, Feb. 2005, pp. 671–87.
[15] V. Eramo, M. Listanti, and A. Germoni, "Cost Evaluation of Optical Packet Switches Equipped With Limited-Range and Full-Range Converters for Contention Resolution," *J. Lightwave Tech.*, vol. 26, no. 4, Feb. 2008, pp. 390–407.
[16] B. Sarker, T. Yoshino, and S. Majumder, "All-Optical Wavelength Conversion Based on Cross-Phase Modulation (XPM) in a Single-Mode Fiber and a Mach-Zehnder Interferometer," *IEEE Photonics Tech. Letters*, vol. 14, no. 3, Mar. 2002, pp. 340–42.
[17] D. Hsu *et al.*, "High-Efficiency Wide-Band SOA-based Wavelength Converters by using Dual-Pumped Four-Wave Mixing and an Assist Beam," *IEEE Photonics Tech. Letters*, vol. 16, Aug. 2004, pp. 1903–5.
[18] J. P. Mack, H. N. Poulsen, and D. J. Blumenthal, "Variable Length Optical Packet Synchronizer," *IEEE Photonics Tech. Letters*, vol. 20, July 2008, pp. 1252–54.
[19] W. Feng and W. D. Zhong, "Noise Analysis of Photonics Packet Synchronizer," *J. Lightwave Tech.*, vol. 22, Feb. 2004, pp. 343–50.
[20] Y. Lin *et al.*, "Using Superimposed ASK Label in a 10 Gb/s Multihop All-Optical Label Swapping System," *J. Lightwave Tech.*, vol. 22, no. 2, Feb. 2004, pp. 351–61.
[21] M. Yuang, P. Tien, and S. Lin, "A Pseudo-Banyan Optical WDM Packet Switching System with Near-Optimal Packet Scheduling," *IEEE/OSA J. Optical Commun. Net.*, vol. 1, no. 3, Aug. 2009, pp. B1–B14.
[22] M. Yuang *et al.*, "QoS Scheduler/Shaper for Optical Coarse Packet Switching IP-over-WDM Networks," *IEEE JSAC*, vol. 22, no. 9, Nov. 2004, pp. 1766–80.
[23] J. Leuthold *et al.*, "All-Optical Mach-Zehnder Interferometer Wavelength Converters and Switches with Integrated Data- and Control-Signal Separation Scheme," *J. Lightwave Tech.*, vol. 17, June 1999, pp. 1056–66.

BIOGRAPHIES

MARIA C. YUANG [SM] (mcyuang@csie.nctu.edu.tw) received her Ph.D. degree in electrical engineering and computer science from Polytechnic University, Brooklyn, New York, in 1989. From 1981 to 1990 she was with AT&T Bell Laboratories and Bell Communications Research (Bellcore), where she was a member of technical staff working on Broadband networks and protocol engineering. In 1990 she joined National Chiao Tung University (NCTU), Taiwan, where she is currently a professor of the Department of Computer Science. She has served as a Guest Editor for *IEEE Journal on Selected Areas in Communications* (Special Issue on Next-Generation Broadband Optical Access Network Technologies) in 2009. She has served on the technical program committees of many technical conferences including IEEE ICC and GLOBECOM, and has been invited to give talks at many technical conferences. Her main research interests include broadband optical networks, wireless networks, multimedia communications, and performance modeling and analysis. She is a member of OSA. She holds 17 patents in the field of broadband networking and has over 100 publications, including a book chapter.

YU-MIN LIN [M] (ymlin5@yahoo.com) received his B.S. degree in electrical engineering from National Tsing-Hua University, Taiwan, in 1996 and his Ph.D. degree in communication engineering from NCTU in 2003. He joined the Department of Optical Communications and Networks, Industrial Technology Research Institute (ITRI), Taiwan, in 2004. His research interests include broadband optical networking and optical packet switching.

JU-LIN SHIH [M] (julin@csie.nctu.edu.tw) received his Ph.D. degree in computer science and information engineering from NCTU in 2006. He joined NCTUniversity in 2006, where he is currently a postdoctoral fellow in the Department of Computer Science. His current research interests include high-speed networking, optical networking, wireless local networking, and performance modeling and analysis.

PO-LUNG TIEN [M] (polungtien@gmail.com) received his B.S. degree in applied mathematics, M.S. degree in computer and information science, and Ph.D. degree in computer science and information engineering from NCTU in 1992, 1995, and 2000, respectively. In 2005 he joined NCTU, where he is currently an assistant professor in the Department of Electrical Engineering. His current research interests include optical networking, computational intelligence, network optimization, multimedia communications, and performance modeling.

JASON (JYEHONG) CHEN [M] (jchen@mail.nctu.edu.tw) received his Ph.D. degree in electrical engineering and computer science from the University of Maryland, Baltimore, in 1998. He joined JDSU in 1998 as a senior engineer and obtained 10 U.S. patents in two years. He joined the faculty of NCTU in 2003, where he is currently an associate professor in the Institute of Electro-Optical Engineering and Department of Photonics.

STEVEN S. W. LEE [M] (steven.sswlee@gmail.com) received his Ph.D. degree in electrical engineering from National Chung Cheng University, Taiwan, in 1999. He joined the Industrial Technology Research Institute (ITRI), Taiwan, in fall 1999, where he was a project leader on optical networking. In 2008 he joined the faculty of National Chung Cheng University, where he is currently an associate professor ub the Department of Communications Engineering. His research interests include optical networks, network planning, and network optimization.

SHIH-HSUAN LIN (shlin@csie.nctu.edu.tw) received his B.S. degree from the Department of Computer Science, National Tsing Hua University, Taiwan, in 2002, and his M.S. degree from the Department of Computer Science, NCTU, in 2004. He is currently working toward his Ph.D. degree in the same department. His research interests include optical networks, wireless data networks, performance modeling and analysis, and optimization theory.

We show simulation results to emphasize that, to achieve higher system scalability with more space-switch clusters, QOPSS can guarantee the same grade of PLP by using a marginally larger buffer size, revealing the economic use of a handful of optical buffers.